Jionoside A1 alleviates ischemic stroke ischemia/reperfusion injury by promoting Nix-mediated mitophagy

Xinyuan Yu[1,2], Xiaojun Liu[2], Xiujuan Mi[2], Xiaoqiong Luo[2], Zhiyun Lian[2], Jun Tang[2,*], Guixue Wang[1*]

[1] Key Laboratory for Biorheological Science and Technology of Ministry of Education, State and Local Joint Engineering Laboratory for Vascular Implants, Bioengineering College of Chongqing University, Chongqing, China

[2] Department of Neurology, Chongqing Hospital of Traditional Chinese Medicine, Chongqing, China

ARTICLE INFO

ABSTRACT

In ischemia-reperfusion injury in ischemic stroke, mitophagy, which can remove damaged mitochondria, reduce cytotoxic damage, and enhance neurological recovery, is crucial. Jionoside A1 is a substance found in the traditional Chinese herb *Rehmannia glutinosa,* which may have neuroprotective effects. The fundamental objective of this work was to find out Jionoside A1's contribution to ischemia/reperfusion injury in ischemic stroke. The oxygen-glucose deprivation/reperfusion (OGD-Rep) model and the right transient middle cerebral artery occlusion (tMCAO) model were established. Jionoside A1 was used for treatment. We utilized a tiny interfering RNA (siRNA) to lower Nix expression. The results suggest that Jionoside A1 may reduce ischemic stroke. By lowering the consequences of ischemia/reperfusion injury, *Rehmannia glutinosa* can be utilized to treat ischemic stroke. These discoveries provide fresh experimental information for the investigation of ischemic stroke ischemia/reperfusion injury and provide some theoretical justification for their application.

Introduction

One of the main causes of disability, stroke results in 44 million disabilities annually throughout the world (1). Ischemic stroke accounts for 80–90% of all cases of stroke. The best treatment for an ischemic stroke right now is a quick return of blood flow. However, following blood reperfusion, brain damage and functional impairment could become worse (2). The process of restoring blood flow and inducing reperfusion injury heeding cerebral ischemia is commonly referred to as cerebral ischemia/reperfusion (I/R) injury. The mitochondrial respiratory chain's function is compromised in the initial stages of ischemia/reperfusion injury (3), and this impairment lasts for at least a week (4,5). When the brain is injured by cerebral ischemia/reperfusion (I/R), mitochondrial damage can result in neuronal death, which affects neural function (6,7). As a result, neuronal damage in ischemic stroke is significantly influenced by mitochondrial damage (8). However, mitophagy can eliminate damaged mitochondria and lessen cytotoxic damage, which encourages the restoration of brain function (9).

In order to protect cells from harm caused by abnormal mitochondrial metabolism and the triggering of apoptosis, mitophagy is a highly specialized mechanism that eliminates malfunctioning or unnecessary mitochondria through the autophagy pathway (10-12). Mitophagy is initiated during the initial stages of ischemia/reperfusion injury, and damaged mitochondria are removed (13-16). Enhancing mitophagy can boost the mitochondrial respiratory chain in neurons, reducing damage to neurons (17-19) and pro-

moting their survival (20,21). Autophagosome creation, the joining of autophagosomes and lysosomes to produce autophagolysosomes, and autophagolysosome digesting are the three primary steps in the mitophagy process. Light chain 3 (LC3) on the autophagosome membrane is activated during the development of autophagosomes and changes from LC3I to LC3II, encouraging the formation of autophagolysosomes (22). The autophagosome and lysosome combination is mediated by P62 and a variety of pathways (23,24), mainly including Parkin-mediated mitophagy, Nix-mediated mitophagy and FUNDC1-mediated mitophagy (25-27).

Jionoside A1, an active compound derived from Rehmannia glutinosa, holds significant promise as a therapeutic agent for the treatment of stroke. Rehmannia glutinosa, a traditional Chinese medication, has long been utilized for its potential in alleviating stroke-related symptoms. Several active components extracted from Rehmannia glutinosa and its analogs have been investigated for their efficacy in treating neurological deficits induced by stroke. Among these components, Jionoside A1 stands out due to its notable cytoprotective properties. Studies have demonstrated that Jionoside A1 exhibits a protective effect against oxidative damage induced by H2O2 in SH-SY5Y cells, suggesting its potential to ameliorate the consequences of cerebral ischemia/reperfusion injury. This finding further supports the notion that Jionoside A1 holds therapeutic value for stroke treatment. By harnessing the neuroprotective properties of Jionoside A1, Rehmannia glutinosa and its active compounds present a promising avenue for the development of stroke interventions. Further research and

investigation are warranted to fully elucidate the underlying mechanisms of action and validate the efficacy of Jionoside A1 in clinical settings. The exploration of Rehmannia glutinosa and its derivatives as potential stroke therapies underscores the significance of traditional medicine in providing alternative treatment options for stroke patients (28-31).

This study looked at how Jionoside A1 affected mitophagy, mitochondrial function, and neuronal function in ischemia/reperfusion injury both in vivo and in vitro, and it went further at the proteins associated to mitophagy that may be involved in mediating this process.

Materials and Methods

Experimental animals

Adult male Sprague-Dawley rats in good health weighing 200–250 g were bought from the Chongqing Medical University Experimental Animal Center (Chongqing, China). Every rat was placed in a spot with a 12-hour cycle of both daylight and darkness, 60% relative humidity, unfettered access to food and drink, and no restrictions. The temperature was maintained at 21–22°C. All experimentation with animals was done with authorization from the Chongqing Medical University Ethics Committee and in accordance with the National Institutes of Health's Guide for the Care and Use of Laboratory Animals.

Culture of primary cortical neurons and an oxygen-glucose deprivation/reperfusion (OGD-Rep) model

We chose Sprague-Dawley rats from Chongqing Medical University's Experimental Animal Center. Cultures of primary neurons in the cortex were carried out as described (32). In a nutshell, rats' cerebral cortices were removed from their bodies 24 hours after birth, their meninges and blood arteries removed, and then they were dissociated by 0.2% papain (LS003119; Worthington Biochemical Corporation, Ohio, USA) for 20 min at 37°C and triturated. The pre-coated plates with poly-L-lysine were loaded with the cell suspensions. The cells were grown in neurobasal-A medium with 2% B27 (21103049 and 17504044; Gibco, Rockville, MD, USA), 0.5 mM glutamine, and 1% antibiotic-antimycotic (HyClone, South Logan, UT, USA) in a humidified incubator at 37°C with 5% CO_2. Every three days, half of the medium was replaced.

The OGD-Rep model was established on the seventh day in vitro (DIV 7). After being thoroughly cleaned with PBS three times, the cultured neurons were put into an anaerobic chamber with 5% CO_2 and 95% N2 and glucose-free DMEM (11966025; Gibco, Rockville, MD, USA) at 37°C for 2 hours. In order to suffer reoxygenation insult, the culture medium was subsequently altered back to the ordinary medium and it remained at 37°C in an incubator with a concentration of 5% carbon dioxide for 12 hours.

Right transient middle cerebral artery occlusion (tMCAO) model

The right tMCAO model was generated as previously described (33). In short, the common carotid artery, external carotid artery (ECA), and internal carotid artery (ICA) are exposed. The tip is advanced from ECA to ICA with paraffin round nylon filament sutures. The filaments are withdrawn for blood reperfusion after 2 hours of congestion. Applying the Longa-Z approach (34), neurological scores were evaluated, and rats who did not demonstrate neurological abnormalities following reperfusion (neurological score 1 or > 3) were not included in the study.

Surgery

Following anesthesia, rats were placed in a stereotaxic apparatus. The right lateral ventricle was punctured with guide cannulas (Plastic One) at the following locations: 1.5 mm laterally to the midline, 0.8 mm posteriorly to the bregma, and 3.8 mm deep (35). Before use, the animals spent 7 days in the animal facility recovering. Daily animal handling was done to inspect the guide cannula and get the rats used to the researchers.

Drug administration

In the OGD-Rep model, a culture medium containing 50 µM Jionoside A1 (HY-N5045 MedChem Express, USA) was administered 1 hour after the model had been set up. After 48 hours, experiments were conducted. Bafilomycin A1 (BafA1) was dissolved in DMSO to prepare a liquor with a concentration of 1 mM and stored at -20°C. The prepared liquor was diluted to a final concentration of 20 µM and introduced to the culture medium two hours before the OGD-Rep model was created.

In the tMCAO model, Jionoside A1 was dissolved in sterile saline, and daily intracerebroventricular injections at a dose of 1 mg/kg were initiated 1 hour following the creation of the tMCAO model. PBS in vitro or sterile saline in vivo in the same dosages were administered to the control groups.

Lentivirus administration

We utilized a tiny interfering RNA (siRNA) with the sequence GGAAGAGTGGAGCCATGAAGA to lower Nix expression. GeneChem Corporation (GeneChem, Shanghai, China) established and developed lentiviral vectors expressing Nix-RNAi (LV-shRNA-Nix). Lentiviral vectors coding for green fluorescent protein (LV-scr-GFP) were used as the control. Neurons were transfected with lentiviruses for 72 hours on DIV 3. Lentiviruses were stereotaxically injected into the right lateral ventricle of rats 7 days before tMCAO. Images were captured by applying a fluorescence microscope (Axio Observer Z1; Carl Zeiss AG, Oberkochen, Germany) for picking up green fluorescence. After transfection with LV-shRNA-Nix, Western blotting was performed to confirm the usefulness of Nix knockdown. The titer of these lentivirus vectors was 5×10^8 transduction units (TU)/ml.

Western blot

A full protein extraction kit (Beyotime, Shanghai, China) was used to extract the protein in its entirety. Using a mitochondrial protein extraction kit (Beyotime, Shanghai, China), mitochondrial proteins were isolated.

Protein was taken out of the OGD-Rep model's or the tMCAO model's peri-ischemic cortical tissues. Using the BCA protein assay reagent (P0010S, Beyotime, Shanghai, China), the protein concentration was determined. All protein samples were denatured by boiling and held at 80°C until analysis. In SDS-PAGE gels, the same amount of protein was injected into each well, electrophoresed in 10% or 12% separating gels, and then transferred to a PVDF membrane. (IPVH00010, Millipore, Billerica, MA, USA). After being blocked with 5% skim milk, the

membranes were then stained with the next set of initial antibodies overnight at 4°C: anti-LC3B(1:500, 18725-1-AP, Proteintech, Wuhan, China), anti-P62 (1:1000, 18420-1-AP, Proteintech, Wuhan, China), anti-TOM20 (1:5000, 11802-1-AP, Proteintech, Wuhan, China), anti-COXIV (1:3000, 11242-1-AP, Proteintech, Wuhan, China), anti-ATP Syn β (1:1000, 17247-1-AP, Proteintech, Wuhan, China), anti-Nix (1:500, 12986-1-AP, Proteintech, Wuhan, China), anti-Parkin (1:500, 14060-1-AP, Proteintech, Wuhan, China), anti-FUNDC1 (1:500, ab224722, Abcam, USA), and anti-GAPDH (1:4000, 60004-1-Ig, Proteintech, Wuhan, China); We used GAPDH as a means of loading control. After cleaning with TBST, the membranes were left to incubate for an hour at room temperature with goat anti-rabbit IgG (1:4000, SA00001-2, Proteintech, Wuhan, China) or anti-mouse IgG (1:4000, SA00001-1, Proteintech, Wuhan, China) antibodies that had been reacted with peroxidase from horseradish. The membranes were subsequently washed with TBST a second time, and an enhanced chemiluminescence (ECL) reagent (P0018FS, Beyotime, Shanghai, China) was used to examine them. A Fusion FX5 analysis tool (Vilber Lourmat, F-77601 Marne-la-Vallée Cedex 3, France) was implemented for capturing the images, and Quantity One software (Bio-Rad Laboratories, Hercules, CA, USA) was utilized for determining the data.

Immunofluorescence

In the OGD-Rep model, MitoTracker CellLight™ Mitochondria-GFP and BacMam 2.0 (C10600, Invitrogen, Carlsbad, CA, USA) were added for 24 hours to the cell medium of culture (3 μl/10,000 cells), and then NeuN staining was performed. 4% paraformaldehyde was applied to fix neurons for 30 min at the temperature of the room, which was followed by 30 min of soaking with 1% Triton X-100 and 1 hour at 37°C of blocking with 5% goat serum (Boster, Wuhan, China). Subsequently, neurons were incubated overnight at 4°C with anti-NeuN antibodies (1:200, 266004, SYSY, USA). Neurons were cleaned with PBS before being treated with the following secondary antibodies for 1 hour at 37°C: DyLight™ 405 AffiniPure goat anti-guinea pig IgG (1:200, AB_2337432, Jackson ImmunoResearch, USA).

In the tMCAO model, rats were intracardially perfused with 0.9% saline and 4% paraformaldehyde. After being removed, the brains were preserved in paraformaldehyde for 24 hours. For immunofluorescence, each fixed brain was frozen and sectioned at a thickness of 10 mm. The frozen portions were dehydrated by immersion in 100% acetone for 20 minutes at room temperature after being air dried at room temperature for 10 minutes. The slices were permeated with 0.4% Triton X-100, wiped three times with PBS, and blocked with ordinary donkey serum for 60 minutes after obtaining the antigen (sections were placed in 10 mM sodium citrate buffer (pH 6.0) and baked in the microwave for 20 min at 92-98°C). Subsequently, the sections were incubated with a mixture of Jiono-NeuN (1:100, 266004, SYSY, USA) and anti-COXIV antibodies (1:50, 11242-1-AP, Proteintech, Wuhan, China) at 4°C overnight. The sections were washed five times with PBS and incubated with a mixture of DyLight™ 405 AffiniPure goat anti-guinea pig IgG (1:200, AB_2337432, Jackson ImmunoResearch, USA) and Alexa Fluor 647-labeled goat anti-mouse IgG (1:100, A0473, Proteintech, Wuhan, China) in

the dark for 60 min at 37°C.fter lentivirus infection transfection, we examined for GFP immunofluorescence in the LV-shRNA-Nix group and the LV-scr-GFP group. The slices were then stained with DAPI before being fixed in a 1:1 glycerol: PBS solution.

Laser scanning confocal microscopy (Leica Microsystems Heidelberg GmbH, Germany) was applied for gathering fluorescence photographs. The samples were protected from light during this procedure to avoid interference with the fluorescent secondary antibody combination during picture acquisition. For the quantitative investigation of expression, mean fluorescence intensity (MFI) was determined for every field of vision using Image-Pro Plus 6.0 (Media Cybernetics, USA).

Measurement of ATP content

Using an ATP assessment kit (S0026, Beyotime, Shanghai, China), ATP content was measured in keeping with the instructions provided by the manufacturer. In short, the homogenates from the OGD-Rep model and the peri-ischemic cortical tissues from the tMCAO model were gathered and centrifuged at 12,000 ×g at 4°C for 5 min. Then, 20 μl of supernatant and 100 μl of ATP detection working solution were mixed, and luminescence was detected with a microplate reader (SpectraMax®i3x, Molecular Devices, USA). The ATP concentration was first quantified according to a standard curve and then normalized to the protein concentration of each experimental group.

Lactate dehydrogenase (LDH) release assay

When the stability of the cell membrane weakens, cytoplasmic LDH flows out, marking the end of the cell (36). According to the manufacturer's instructions, we measured LDH release using an LDH Cytotoxicity Assay Kit (Proteintech, Wuhan, China). In simpler terms, 20 μl of the releasing LDH reagent from the kit was put into the cell culture well, and the cells were then left to incubate for an hour. The cell culture dish was subsequently spun for 5 minutes at 400×g. Next, 120 μl of supernatant from each well was added to the corresponding wells of a new 96-well plate, and 60 μl of LDH detection working solution was then added to each well of the 96-well plate. The 96-well plate underwent incubation for 30 minutes in a darkroom at room temperature. The maximum amount of LDH release per well was calculated using the absorption reading at 490 nm.

Neurobehavioral assessment

The modified neurological severity score (mNSS) was calculated 3 days before and 1, 7 and 14 days after tMCAO. The mNSS is an amalgamated test of equilibrium, reaction, motor, and sensory skills. Ratings for neuronal function varied from 0 to 18 (normal score, 0; maximal deficit score, 18). The absence of the reflex being investigated or the inability to perform the examination is represented by a point in the injury severity ratings (37). Each trial was separated by a minimum of 5 min. Animals were trained for 3 days prior to tMCAO (38).
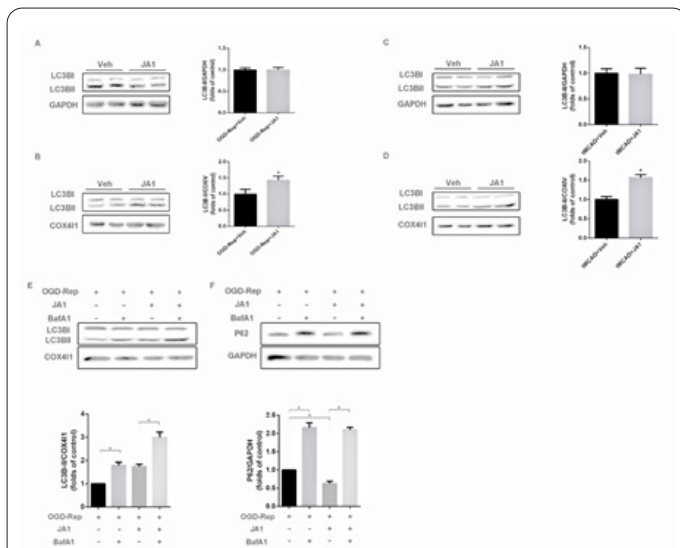
Statistical analysis

Statistic Package for Social Science (SPSS) 20.0 software (IBM, Armonk, NY, USA) was used for all statistical analyses. Data are shown as mean ± standard error of the mean (SEM). The Shapiro-Wilk normality test was

used to determine whether the data had a normal distribution, and Levene's test for homogeneity of variance was used to assess variance. A two-way repeated measures analysis of variance (ANOVA) with a Bonferroni post hoc test was used to analyze the effect of treatment on the mNSS score. Student's t-test and ANOVA with Bonferroni's post hoc test were implemented to analyze information with an equal variance; in cases of unequal variance in the data, one-way ANOVA with Dunnett's T3 post-hoc test was performed. Values of $P < 0.05$ were considered to indicate statistical significance.

Results

Jionoside A1 promoted mitophagy in ischemic stroke ischemia/reperfusion injury

In order to observe the impact of Jionoside A1 on mitophagy in ischemia/reperfusion injury, we evaluated the cellular and mitochondrial expression levels of LC3BII in the OGD-Rep model and the tMCAO model, respectively. Jionoside A1 dramatically raised LC3BII expression at the mitochondrial level in the OGD-Rep model after 48 hours of treatment, but it had no discernible impact on LC3BII expression at the neuronal level (Figure 1A-B). After 14 days of treatment in the tMCAO model, Jionoside A1 likewise dramatically raised the expression of LC3BII at the mitochondrial level, but it had no discernible impact on the expression of LC3BII at the cellular level (Figure

1C-D). This finding suggested that Jionoside A1 may encourage mitophagy in the injury caused by an ischemic stroke and ischemia/reperfusion.

The effect of Jionoside A1 on mitophagy flux was also demonstrated in the OGD-Rep model by blocking autophagy at the late stage with the highly specific vacuolar H+-ATPase (V-ATPase) inhibitor BafA1. Jionoside A1 downregulated the neuronal expression of P62 while still considerably increasing the mitochondrial expression of LC3BII under the influence of BafA1 (Figure 1E, F). Furthermore, regardless of whether Jionoside A1 was used, BafA1 dramatically elevated the neuronal expression of P62 (Figure 1F). This finding revealed that Jionoside A1 boosted the mitochondrial expression of LC3BII in ischemic stroke ischemia/reperfusion injury by increasing mitophagy levels rather than by preventing the degradation process.

Jionoside A1 increased mitochondrial content in ischemic stroke ischemia/reperfusion injury

Jionoside A1 considerably increased after 48 hours of treatment the neuronal expression of the mitochondrial marker proteins TOMM20, COX4I1 and ATP Synβ in the OGD-Rep model (Figure 2A, B). In the tMCAO model,
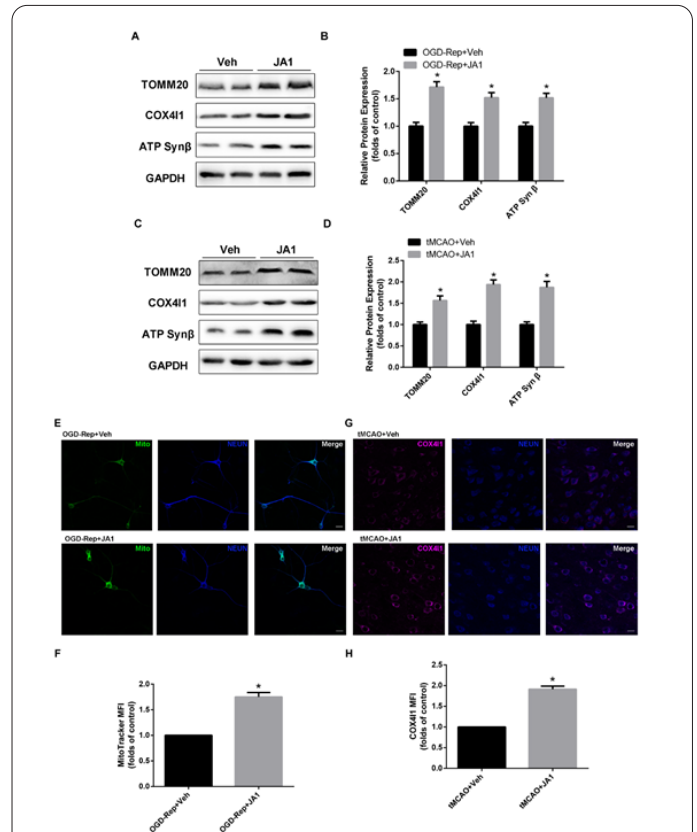

Figure 1. Effect of Jionoside A1 on mitophagy in ischemia/reperfusion injury. (A) Representative images (left) and statistical analysis results (right) of LC3B expression at the neuronal level in the OGD-Rep model (P>0.05, unpaired t-test, n=5). (B) Representative images (left) and statistical analysis results (right) of LC3B expression at the mitochondrial level in the OGD-Rep model (*P<0.05, unpaired t-test, n=5). (C) Representative images (left) and statistical analysis results (right) of LC3B expression at the cellular level in the tMCAO model (P>0.05, unpaired t-test, n=5). (D) Representative images (left) and statistical analysis results (right) of LC3B expression at the mitochondrial level in the tMCAO model (*P<0.05, unpaired t-test, n=5). (E) Representative images (top) and statistical analysis results (bottom) of LC3B expression under the effect of BafA1 at the mitochondrial level in the OGD-Rep model (*P<0.05, one-way ANOVA, n=5). (F) Representative images (top) and statistical analysis results (bottom) of P62 expression under the effect of BafA1 at the neuronal level in the OGD-Rep model (*P<0.05, one-way ANOVA, n=5).

Figure 2. Effect of Jionoside A1 on mitochondrial content in ischemia/reperfusion injury. (A-B) Representative images (A) and statistical analysis results (B) of TOMM20, COX4I1 and ATP Synβ expression in the OGD-Rep model (*P<0.05, unpaired t-test, n=5). (C-D) Representative images (C) and statistical analysis results (D) of TOMM20, COX4I1 and ATP Synβ expression in the tMCAO model (*P<0.05, unpaired t-test, n=5). (E-F) Representative images (E) and statistical analysis results (F) of double immunofluorescence of Mito-Tracker CellLight™ Mitochondria-GFP (green) and NeuN (blue) (scale bar=50 μm, *P<0.05, unpaired t-test, n=5). (G-H) Representative images (G) and statistical analysis results (H) of double immunofluorescence of COX4I1 (pink) and NeuN (blue) (scale bar=50 μm, *P<0.05, unpaired t test, n=5).
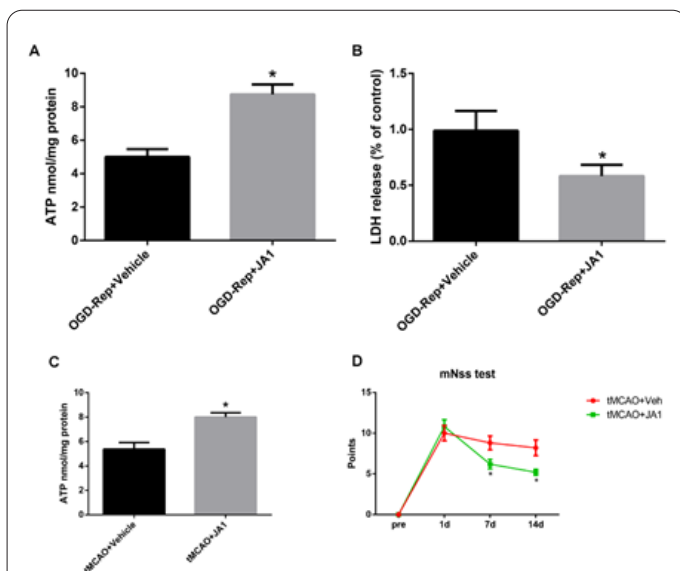
Jionoside A1 also markedly raised the cellular expression of TOMM20, COX4I1 and ATP Synβ after 14 days of application (Figure 2C, D). The OGD-Rep model after 48 hours of administration (Figure 2E, F) and the tMCAO model after 14 days of application (Figure 2G, H) both demonstrated considerably higher mitochondrial content upon immunofluorescence detection. According to this finding, ischemic stroke victims who had suffered ischemia/reperfusion injury had more mitochondria.

Jionoside A1 increased ATP levels, reduced neuronal cytotoxicity, and improved neurobehavior in ischemic stroke ischemia/reperfusion injury
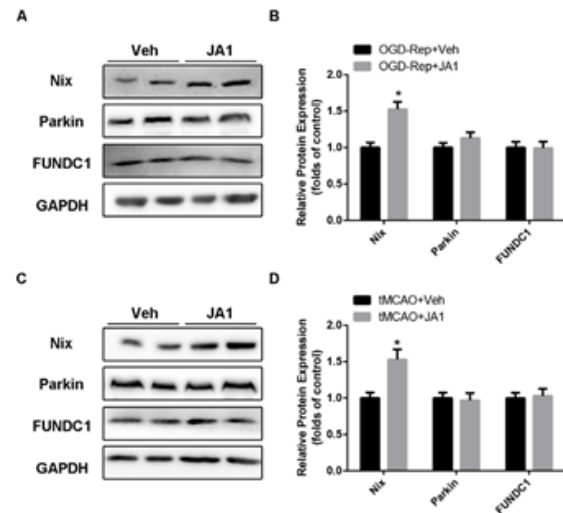
In the OGD-Rep model after 48 hours of administration (Figure 3A) and in the tMCAO model after 14 days of application, the cellular ATP level considerably increased. In the OGD-Rep model, the release of LDH was greatly reduced, which suggested lessened neuronal cytotoxicity (Figure 3B-C). The mNSS score was used in the tMCAO model to measure neurobehavioral function, and the results showed that the mNSS score of the tMCAO model rats dramatically decreased at days 7 and 14 after Jionoside A1 treatment (Figure 3D). According to these findings, Jionoside A1 reduces ischemia/reperfusion damage in ischemic stroke.

Jionoside A1 upregulated Nix expression in ischemic stroke ischemia/reperfusion injury

To investigate the key mitophagy-related proteins related to Jionoside A1 in ischemia/reperfusion injury, the expression of Parkin, Nix and FUNDC1 was determined in both the OGD-Rep and tMCAO models. In the OGD-Rep model, Jionoside A1 significantly increased the neu-

Figure 4. Effect of Jionoside A1 on the levels of key mitophagy-related proteins in ischemia/reperfusion injury. (A-B) Representative images (A) and statistical analysis results (B) of Parkin, Nix and FUNDC1 expression in the OGD-Rep model (*P<0.05, unpaired t-test, n=5). (C-D) Representative images (C) and statistical analysis results (D) of Parkin, Nix and FUNDC1 expression in the tMCAO model (*P<0.05, unpaired t-test, n=5).
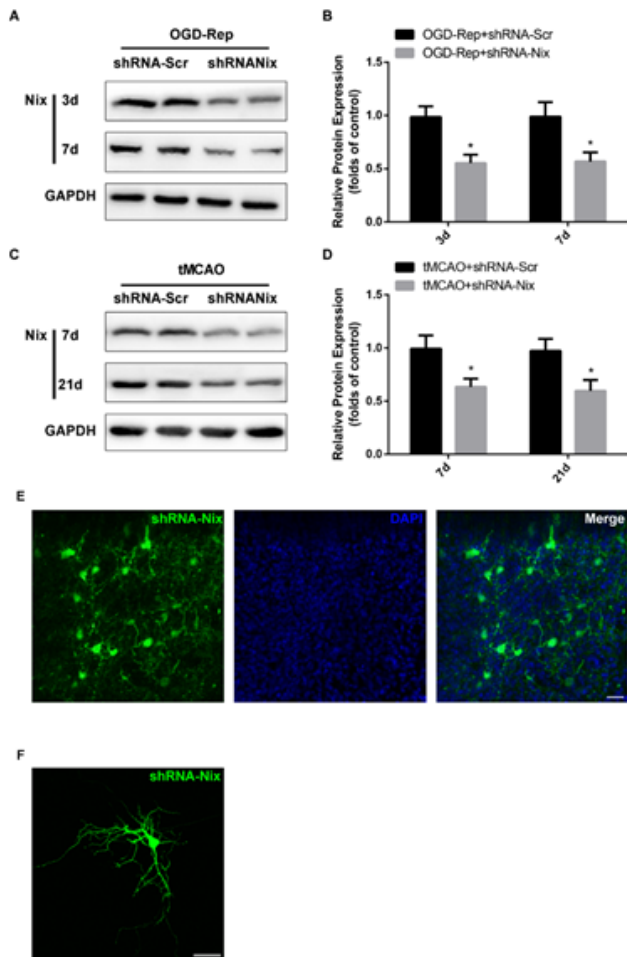
ronal expression of Nix after 48 h of application, while the expression levels of Parkin and FUNDC1 showed no significant change (Figure 4A, B). In the tMCAO model, similar expression changes were also observed in the cortex near the infarct area (Figure 4C, D). This specific effect of Jionoside A1 on Nix suggested that Nix-mediated mitophagy may play an important role in Jionoside A1-mediated alleviation of ischemia/reperfusion injury.

Analysis of Nix expression after transfection of recombinant lentivirus

Cell culture medium containing LV-shRNA-Nix or LV-scr-GFP was added to DIV3 primary cortical neurons, and the transfection efficiency was measured on day 3 and day 7 after transfection. The neuronal expression of Nix was significantly decreased in the LV-shRNA-Nix group compared with that in the LV-scr-GFP group on days 3 and 7 (Figure 5A, B). This outcome demonstrated that the neurons had been successfully transduced with LV-shRNA-Nix, which had effectively decreased Nix expression. LV-shRNA-Nix and LV-scr-GFP were injected into the right lateral ventricle of rats. The transfection efficiency was measured on day 7 and day 21 after lentivirus injection. In the cortex near the right lateral ventricle, the expression of Nix was significantly decreased in the LV-shRNA-Nix group compared with that in the LV-scr-GFP group on days 7 and 21 (Figure 5C, D). Additionally, LV loaded with GFP was observed in the neurons of the cortex near the right lateral ventricle (Figure 5E). Additionally, LV loaded with GFP was observed in the neurons (Figure 5F). This study demonstrated that Nix expression has been effectively decreased by LV-shRNA-Nix transmission into the neurons of the cortex close to the right lateral ventricle.
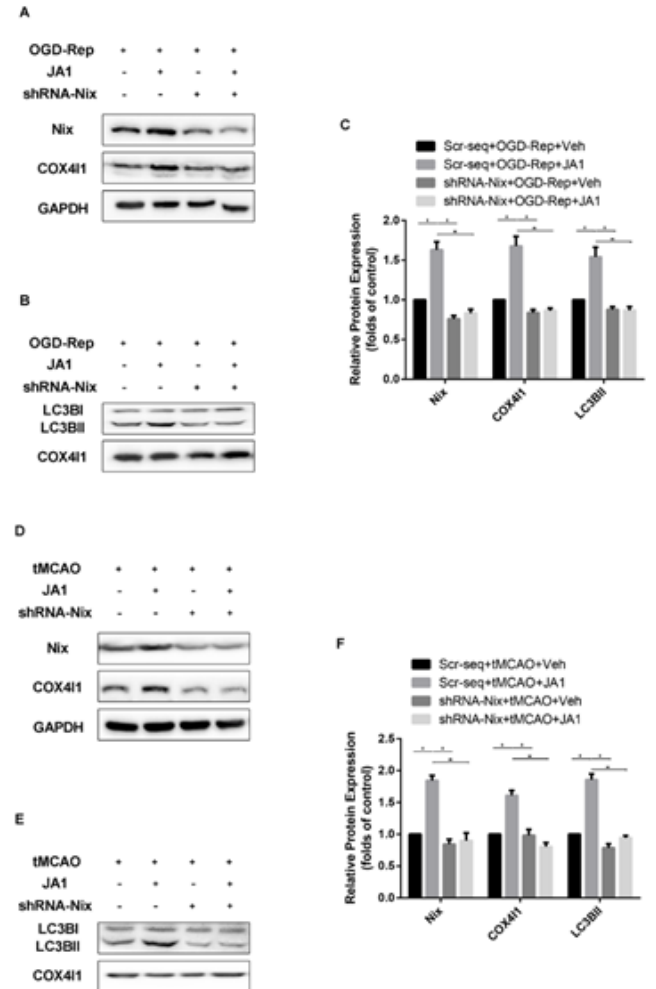
Knockdown of Nix attenuates Jionoside A1-mediated promotion of mitophagy and mitochondrial content in ischemic stroke ischemia/reperfusion injury

To investigate whether Nix knockdown suppresses

Figure 3. Effect of Jionoside A1 on ATP levels, LDH release, and neurobehavior in ischemia/reperfusion injury. (A) The cellular ATP level was increased in OGD-Rep + JA1 group compared with that in the OGD-Rep + Vehicle group (*P<0.05, unpaired t-test, n=5). (B) The release of LDH decreased in OGD-Rep + JA1 group compared with that in the OGD-Rep + Vehicle group (*P<0.05, unpaired t-test, n=5). (C) The ATP level was increased in tMCAO + JA1 group compared with that in the tMCAO + Vehicle group (*P<0.05, unpaired t-test, n=5). (D) The mNSS score was decreased in tMCAO + JA1 group compared with that in the tMCAO + Vehicle group on day 7 and day 14 (*P<0.05, two-way ANOVA, n=9).

Figure 5. Expression of Nix with a green fluorescent protein (GFP) after transfection of a recombinant LV and its effects in primary cortical neurons and the cortex near the right lateral ventricle. (A-B) Representative images (A) and statistical analysis results (B) showing Nix expression in primary cortical neurons with or without transfection of LV-scr-GFP and LV-shRNA-Nix on day 3 and day 7 (*P<0.05, unpaired t-test, n=5). (C-D) Representative images (C) and statistical analysis results (D) showing Nix expression in the cortex near the right lateral ventricle with or without injection of LV-scr-GFP and LV-shRNA-Nix on day 7 and day 21 (*P<0.05, unpaired t-test, n=5). (E-F) Immunofluorescence images showing GFP expression in primary cortical neurons after 7 days (E) and in the cortex near the right lateral ventricle after 21 days (F) of transfection of recombinant LV (scale bar=100 μm).
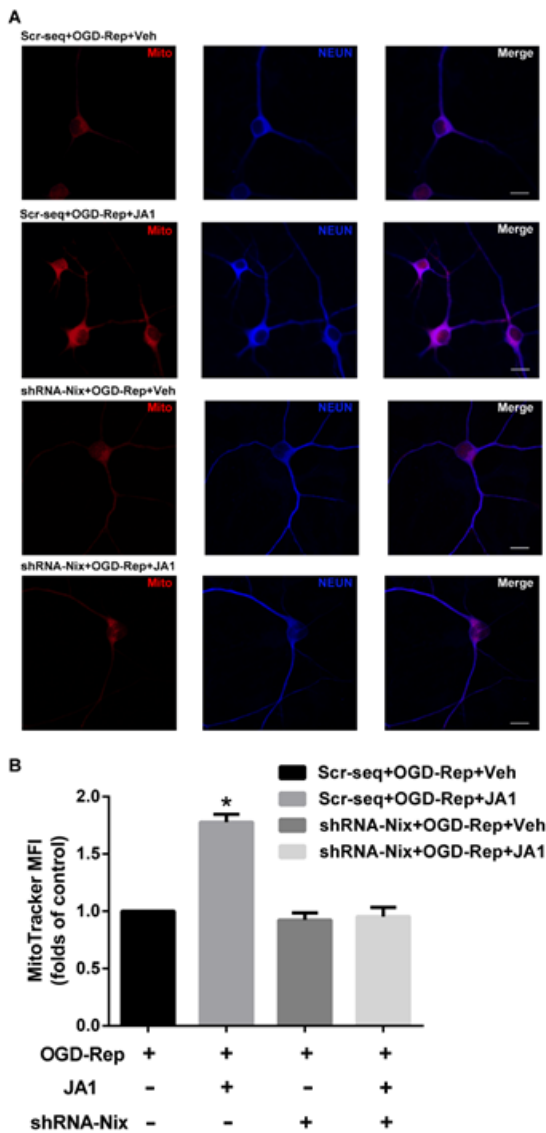

Figure 6. Jionoside A1 fails to induce mitophagy and mitochondrial content with Nix knockdown. (A-C) Representative images (A-B) and statistical analysis results (C) showing LC3B expression at the mitochondrial level and COX4I1 expression at the neuronal level with administration of Jionoside A1 after Nix knockdown in the OGD-Rep model (*P<0.05, one-way ANOVA, n=5). (D-F) Representative images (D-E) and statistical analysis results (F) showing LC3B expression at the mitochondrial level and COX4I1 expression at the cellular level with administration of Jionoside A1 after Nix knockdown in the tMCAO model (*P<0.05, one-way ANOVA, n=5).

Jionoside A1-mediated promotion of mitophagy and mitochondrial content, we pretreated primary cortical neurons with cell culture medium containing LV-shRNA-Nix or LV-scr-GFP 3 days before OGD-Rep model establishment. Continuous administration of Jionoside A1 was conducted 1 h after OGD-Rep model establishment. The expression of mitochondrial LC3BII and neuronal COX4I1 was detected after 48 h of Jionoside A1 application. After downregulating the expression of Nix, the Jionoside A1-mediated upregulation of mitochondrial LC3BII and neuronal COX4I1 in the OGD-Rep model was attenuated (Figure 6A-C). We also pretreated rats with LV-shRNA-Nix or LV-scr-GFP 7 days before tMCAO model establishment. The repeated administration of Jionoside A1 was conducted 1 h after the tMCAO model establishment. The expression of mitochondrial LC3BII and cellular COX4I1 was detected after 14 days of Jionoside A1 application. After downregu-

lating the expression of Nix, Jionoside A1-mediated upregulation of mitochondrial LC3BII and cellular COX4I1 in the tMCAO model was attenuated (Figure 6D-F). Immunofluorescence detection was also conducted to determine the effect of Jionoside A1 on mitochondrial content after Nix knockdown in the OGD-Rep model. Jionoside A1 upregulation of mitochondrial content was attenuated after downregulating Nix expression (Figure 7). These results indicated that Jionoside A1 may increase mitochondrial content via Nix-mediated mitophagy in ischemic stroke ischemia/reperfusion injury.

Knockdown of Nix attenuates the effect of Jionoside A1 on ATP levels, neuronal cytotoxicity, and neurobehavior in ischemic stroke ischemia/reperfusion injury

Whether Nix knockdown suppresses the effect of Jionoside A1 on ATP levels, neuronal cytotoxicity, and neurobehavior was further investigated. After downregulating the expression of Nix, Jionoside A1 upregulation of cellular ATP levels was attenuated in both the OGD-Rep

Figure 7. Jionoside A1 fails to increase mitochondrial content with Nix knockdown. (A) Representative images of double immunofluorescence of Mito-Tracker CellLight™ Mitochondria-GFP (green) and NeuN (blue) (scale bar=50 μm). (B) Statistical analysis results of double immunofluorescence of Mito-Tracker CellLight™ Mitochondria-GFP (*P<0.05, one-way ANOVA, n=5).

drial expression of LC3BII but not the cellular expression of LC3BII. Yet, the enhanced binding of LC3BII to mitochondria after autophagy activation or the failure of mitochondrial autophagosome clearance may be the reason for the increased LC3BII expression in mitochondria. The impact of Jionoside A1 on mitophagy flow was also noted in the OGD-Rep model, which helps to further explain these hypotheses. When blocking autophagy at the late stage with BafA1, Jionoside A1 still significantly increased the mitochondrial expression of LC3BII. This result suggests that autophagosome clearance is not blocked by the Jionoside A1 administration. Thus, we focused on the influence of Jionoside A1 on autophagosome formation.

According to this study, Jionoside A1 treatment raised the levels of the mitochondrial markers TOMM20, COX4I1, and ATP Syn β. TOMM20 is a mitochondrial outer membrane protein essential for mitochondrial protein import machinery (39). COX4I1 is a mitochondrial inner membrane protein essential for the mitochondrial respiratory chain (39,40). ATP Syn β is also a mitochondrial inner membrane protein that is closely related to ATP synthesis (41). Therefore, the upregulation of TOMM20, COX4I1 and ATP Syn β by Jionoside A1 reflects not only the increase in mitochondrial content but also the improvement in mitochondrial function, which is consistent with the results of the ATP content measurement.

In the early stage of ischemic stroke ischemia/reperfusion injury, enhancing mitophagy can improve the function of the mitochondrial respiratory chain and alleviate neuronal damage (17-19). Therefore, in order to enhance the recovery of neurological function after an ischemic stroke, mitophagy may be a viable pharmacological target.

As described previously (25-27), the regulation of autophagosome formation is primarily mediated by three mitophagy-related proteins. These mitophagy-related proteins participate in the regulation of Parkin-mediated mitophagy, Nix-mediated mitophagy and FUNDC1-mediated mitophagy. Jionoside A1 administration produced a specific increase in the expression of Nix, which suggests that Nix-mediated mitophagy may play an important role in Jionoside A1-mediated alleviation of ischemia/reperfu-

(Figure 8A) and tMCAO models (Figure 8B). In the OGD-Rep model, Jionoside A1-mediated downregulation of LDH release was also attenuated (Figure 8C). Moreover, Jionoside A1-mediated reduction in the mNSS score was also attenuated in the tMCAO model (Figure 8D). These results suggested that Jionoside A1 alleviates ischemic stroke ischemia/reperfusion injury by promoting Nix-mediated mitophagy.

Discussion

These findings demonstrate that Jionoside A1 alleviates ischemia/reperfusion injury in ischemic stroke, stimulates mitophagy, and enhances mitochondrial content. Nix knockdown attenuates these effects of Jionoside A1 in ischemic stroke ischemia/reperfusion injury, which indicates that Nix-mediated mitophagy may be involved in this process.
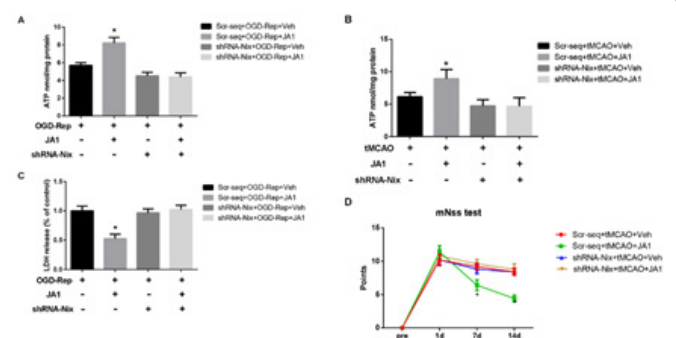
Jionoside A1 may selectively stimulate mitophagy because this study found that it could boost the mitochon-

Figure 8. Jionoside A1 fails to affect ATP levels, LDH release, or neurobehavior with Nix knockdown. (A) Statistical analysis results of the cellular ATP level after Nix knockdown in the OGD-Rep model (*P<0.05, one-way ANOVA, n=5). (B) Statistical analysis results of LDH release after Nix knockdown in the OGD-Rep model (*P<0.05, one-way ANOVA, n=5). (C) Statistical analysis results of the cellular ATP level after Nix knockdown in the tMCAO model (*P<0.05, one-way ANOVA, n=5). (D) Statistical analysis results of the mNSS score after Nix knockdown in the tMCAO model (*P<0.05, two-way ANOVA, n=9).

sion injury (42).

Nix is a mitochondrial membrane receptor that mediates the formation of autophagosomes in mitophagy and is also related to mitophagy in hypoxia (22). Under hypoxic conditions, Nix-mediated mitophagy is easily activated and combines mitochondria and autophagic vesicles through LC3 to form autophagosomes, thereby promoting mitophagy (22,25,27). In ischemia/reperfusion injury, Nix-mediated mitophagy can independently protect against ischemic brain injury and promote the functional recovery of cerebral ischemia-reperfusion tissues (27). This study showed that Nix knockdown attenuated the effect of Jionoside A1 on mitophagy and mitochondrial content and further attenuated the protective effect of Jionoside A1 in ischemia/reperfusion injury. This finding suggests that Jionoside A1 alleviates ischemic stroke ischemia/reperfusion injury by promoting Nix-mediated mitophagy.

Despite the fact that this work demonstrates that Jionoside A1 can reduce ischemic stroke ischemia/reperfusion injury by encouraging Nix-mediated mitophagy, Jionoside A1's protective effects are probably not exclusive to this pathway. In the process of ischemic stroke ischemia/reperfusion injury, many damaged mitochondria emerge (4,5). The increase in mitochondrial content under Jionoside A1 administration may also be accompanied by accelerated mitochondrial biogenesis, which could be caused by Jionoside A1 administration or a compensatory effect of mitophagy activation. Further study may be needed to clarify this phenomenon.

Our comprehensive findings presented in this study highlight the potential therapeutic benefits of Jionoside A1 in mitigating the detrimental effects of ischemic stroke and the associated ischemia/reperfusion injury. The results provide compelling evidence for the role of Jionoside A1 in activating the Nix-mediated mitophagy pathway, which contributes to the reduction of ischemic damage. The observed neuroprotective effects of Jionoside A1 hold significant implications for ischemic stroke research and offer promising avenues for the development of novel therapeutic interventions. By unraveling the molecular mechanisms underlying its action, this study sheds light on the potential use of Rehmannia glutinosa as a valuable resource for addressing ischemic stroke-related complications. The activation of mitophagy, particularly through the Nix pathway, appears to be a crucial mechanism by which Jionoside A1 exerts its protective effects. By selectively removing damaged mitochondria, Jionoside A1 facilitates cellular homeostasis and prevents the accumulation of harmful reactive oxygen species and pro-inflammatory mediators, thereby preserving neuronal integrity. These findings not only advance our understanding of the pathophysiology of ischemic stroke but also pave the way for the development of targeted therapeutic strategies. The identification of Jionoside A1 as a potential neuroprotective agent offers exciting prospects for future preclinical and clinical investigations, aiming to validate its efficacy and safety in human subjects.

Conclusion

In summary, this study contributes novel insights into the protective effects of Jionoside A1 against ischemic stroke-induced injury, emphasizing the importance of Nix-mediated mitophagy in this process. These findings hold promise for the development of innovative treatments for ischemic stroke, bringing us closer to effective interventions that can improve patient outcomes and reduce the burden of this debilitating condition.

References

1. Khoshnam SE, Winlow W, Farzaneh M, Farbood Y, Moghaddam HF. Pathogenic mechanisms following ischemic stroke. Neurol Sci 2017; 38(7): 1167-1186.

2. Chomova M, Zitnanova I. Look into brain energy crisis and membrane pathophysiology in ischemia and reperfusion. Stress 2016; 19(4): 341-348.

3. Chen X, Xie Y, Liang C, Yang D, Li X, Yu J. Tug1 Acts on ERK12 Signaling Pathway to Aggravate Neuronal Damage after Acute Ischemic Stroke. Cell Mol Biol 2022; 68(1): 51-58.

4. Bi J, Li H, Ye SQ, Ding S. Pre-B-cell colony-enhancing factor exerts a neuronal protection through its enzymatic activity and the reduction of mitochondrial dysfunction in in vitro ischemic models. J Neurochem 2012; 120(2): 334-346.

5. Chen Z, Wang N, Na R, et al. Bioinformatic prediction of depression-related signaling pathways regulated by miR-146a in peripheral blood of patients with post-stroke depression. Cell Mol Biol 2022; 68(6): 40-47.

6. Wang Y, Li X, Liu Y, et al. Notch3 Mutation Detection in Stroke Patients and Selective Nanoliposome in Stroke Alleviation in a Mouse Model. J Biomed Nanotechnol 2021; 17(9): 1735-1744.

7. Wang Z, Ye Z, Huang G, Wang N, Wang E, Guo Q. Sevoflurane Post-conditioning Enhanced Hippocampal Neuron Resistance to Global Cerebral Ischemia Induced by Cardiac Arrest in Rats through PI3K/Akt Survival Pathway. Front Cell Neurosci 2016; 10(271.

8. Wei Y, Zhang J. Adoption of Manganese-Doped Copper Sulfide Nanodot-Based Multimodal Magnetic Resonance Imaging in Prognosis Prediction of Patients with Ischemic Stroke Under Nutritional Care. J Biomed Nanotechnol 2022; 18(6): 1620-1629.

9. Kubli DA, Gustafsson AB. Mitochondria and mitophagy: the yin and yang of cell death control. Circ Res 2012; 111(9): 1208-1221.

10. Yao Z, Wood NW. Cell death pathways in Parkinson's disease: role of mitochondria. Antioxid Redox Sign 2009; 11(9): 2135-2149.

11. Shi ZH, Nie G, Duan XL, et al. Neuroprotective mechanism of mitochondrial ferritin on 6-hydroxydopamine-induced dopami-

nergic cell damage: implication for neuroprotection in Parkinson's disease. Antioxid Redox Sign 2010; 13(6): 783-796.

12. Lim KL, Ng XH, Grace LG, Yao TP. Mitochondrial dynamics and Parkinson's disease: focus on parkin. Antioxid Redox Sign 2012; 16(9): 935-949.

13. Zhang X, Yan H, Yuan Y, et al. Cerebral ischemia-reperfusion-induced autophagy protects against neuronal injury by mitochondrial clearance. Autophagy 2013; 9(9): 1321-1333.

14. Li Q, Zhang T, Wang J, et al. Rapamycin attenuates mitochondrial dysfunction via activation of mitophagy in experimental ischemic stroke. Biochem Bioph Res Co 2014; 444(2): 182-188.

15. Zuo W, Zhang S, Xia CY, Guo XF, He WB, Chen NH. Mitochondria autophagy is induced after hypoxic/ischemic stress in a Drp1 dependent manner: the role of inhibition of Drp1 in ischemic brain damage. Neuropharmacology 2014; 86: 103-115.

16. Yu S, Zheng S, Leng J, Wang S, Zhao T, Liu J. Inhibition of mitochondrial calcium uniporter protects neurocytes from ischemia/reperfusion injury via the inhibition of excessive mitophagy. Neurosci Lett 2016; 628: 24-29.

17. Silachev DN, Plotnikov EY, Zorova LD, et al. Neuroprotective Effects of Mitochondria-Targeted Plastoquinone and Thymoquinone in a Rat Model of Brain Ischemia/Reperfusion Injury. Molecules 2015; 20(8): 14487-14503.

18. Nguyen H, Zarriello S, Rajani M, Tuazon J, Napoli E, Borlongan CV. Understanding the Role of Dysfunctional and Healthy Mitochondria in Stroke Pathology and Its Treatment. Int J Mol Sci 2018; 19(7):

19. Flippo KH, Gnanasekaran A, Perkins GA, et al. AKAP1 Protects from Cerebral Ischemic Stroke by Inhibiting Drp1-Dependent Mitochondrial Fission. J Neurosci 2018; 38(38): 8233-8242.

20. Li J, Lu J, Mi Y, et al. Voltage-dependent anion channels (VDACs) promote mitophagy to protect neuron from death in an early brain injury following a subarachnoid hemorrhage in rats. Brain Res 2014; 1573: 74-83.

21. Zhang X, Yuan Y, Jiang L, et al. Endoplasmic reticulum stress induced by tunicamycin and thapsigargin protects against transient ischemic brain injury: Involvement of PARK2-dependent mitophagy. Autophagy 2014; 10(10): 1801-1813.

22. Lou G, Palikaras K, Lautrup S, Scheibye-Knudsen M, Tavernarakis N, Fang EF. Mitophagy and Neuroprotection. Trends Mol Med 2020; 26(1): 8-20.

23. Narendra D, Tanaka A, Suen DF, Youle RJ. Parkin is recruited selectively to impaired mitochondria and promotes their autophagy. J Cell Biol 2008; 183(5): 795-803.

24. Joassard OR, Amirouche A, Gallot YS, et al. Regulation of Akt-mTOR, ubiquitin-proteasome and autophagy-lysosome pathways in response to formoterol administration in rat skeletal muscle. Int J Biochem Cell B 2013; 45(11): 2444-2455.

25. Tracy K, Dibling BC, Spike BT, Knabb JR, Schumacker P, Macleod KF. BNIP3 is an RB/E2F target gene required for hypoxia-induced autophagy. Mol Cell Biol 2007; 27(17): 6229-6242.

26. Evans TD, Sergin I, Zhang X, Razani B. Target acquired: Selective autophagy in cardiometabolic disease. Sci Signal 2017; 10(468):

27. Yuan Y, Zheng Y, Zhang X, et al. BNIP3L/NIX-mediated mitophagy protects against ischemic brain injury independent of PARK2. Autophagy 2017; 13(10): 1754-1766.

28. Xu N, Huang F, Jian C, et al. Neuroprotective effect of salidroside against central nervous system inflammation-induced cognitive deficits: A pivotal role of sirtuin 1-dependent Nrf-2/HO-1/NF-kappaB pathway. Phytother Res 2019; 33(5): 1438-1447.

29. Liu Y, Xue Q, Li X, et al. Amelioration of stroke-induced neurological deficiency by lyophilized powder of catapol and puerarin. Int J Biol Sci 2014; 10(4): 448-456.

30. Biswal S, Barhwal KK, Das D, et al. Salidroside mediated stabilization of Bcl -x(L) prevents mitophagy in CA3 hippocampal neurons during hypoxia. Neurobiol Dis 2018; 116: 39-52.

31. Shen L, Chen H, Zhu Q, et al. Identification of bioactive ingredients with immuno-enhancement and anti-oxidative effects from Fufang-Ejiao-Syrup by LC-MS(n) combined with bioassays. J Pharmaceut Biomed 2016; 117: 363-371.

32. Beaudoin GR, Lee SH, Singh D, et al. Culturing pyramidal neurons from the early postnatal mouse hippocampus and cortex. Nat Protoc 2012; 7(9): 1741-1754.

33. Zhang K, Zhang Q, Deng J, et al. ALK5 signaling pathway mediates neurogenesis and functional recovery after cerebral ischemia/reperfusion in rats via Gadd45b. Cell Death Dis 2019; 10(5): 360.

34. Longa EZ, Weinstein PR, Carlson S, Cummins R. Reversible middle cerebral artery occlusion without craniectomy in rats. Stroke 1989; 20(1): 84-91.

35. Zhou P, Homberg JR, Fang Q, et al. Histamine-4 receptor antagonist JNJ7777120 inhibits pro-inflammatory microglia and prevents the progression of Parkinson-like pathology and behaviour in a rat model. Brain Behav Immun 2019; 76: 61-73.

36. Lobner D. Comparison of the LDH and MTT assays for quantifying cell death: validity for neuronal apoptosis? J Neurosci Meth 2000; 96(2): 147-152.

37. Chen J, Sanberg PR, Li Y, et al. Intravenous administration of human umbilical cord blood reduces behavioral deficits after stroke in rats. Stroke 2001; 32(11): 2682-2688.

38. Shen LH, Li Y, Chen J, et al. One-year follow-up after bone marrow stromal cell treatment in middle-aged female rats with stroke. Stroke 2007; 38(7): 2150-2156.

39. Wiedemann N, Pfanner N. Mitochondrial Machineries for Protein Import and Assembly. Annu Rev Biochem 2017; 86: 685-714.

40. Hess KC, Liu J, Manfredi G, et al. A mitochondrial CO2-adenylyl cyclase-cAMP signalosome controls yeast normoxic cytochrome c oxidase activity. Faseb J 2014; 28(10): 4369-4380.

41. Cha MY, Cho HJ, Kim C, et al. Mitochondrial ATP synthase activity is impaired by suppressed O-GlcNAcylation in Alzheimer's disease. Hum Mol Genet 2015; 24(22): 6492-6504.

42. Tang YC, Tian HX, Yi T, Chen HB. The critical roles of mitophagy in cerebral ischemia. Protein Cell 2016; 7(10): 699-713.